

# Structure determination of rubredoxin from *Desulfovibrio vulgaris* Miyazaki F in two crystal forms

Shintaro Misaki,<sup>a</sup> Yukio Morimoto,<sup>a</sup> Mari Ogata,<sup>b</sup> Tatsuhiko Yagi,<sup>b</sup> Yoshiki Higuchi<sup>c\*</sup> and Noritake Yasuoka<sup>a</sup>

<sup>a</sup>Department of Life Science, Faculty of Science, Himeji Institute of Technology, Kanaji 1475-2, Kamigori, Ako-gun, Hyogo 678-1297, Japan, <sup>b</sup>Shizuoka University, 836 Oya, Shizuoka 422-8529, Japan, and <sup>c</sup>Division of Chemistry, Graduate School of Science, Kyoto University, Sakyo, Kyoto 606-8502, Japan

Correspondence e-mail:  
higuchi@kuchem.kyoto-u.ac.jp

The structures of two crystal forms (form I,  $P3_221$ ,  $a = b = 43.7$ ,  $c = 50.7$  Å; form II,  $P2_1$ ,  $a = 27.3$ ,  $b = 44.9$ ,  $c = 51.2$  Å and  $\beta = 90.6^\circ$ ) of the rubredoxin from *Desulfovibrio vulgaris* Miyazaki F have been solved by the molecular-replacement method. Form I has been refined at a resolution of 2.0 Å to an  $R$  value of 20.8% and includes 32 water molecules. Form II includes 86 water molecules and has been refined at 1.9 Å resolution to an  $R$  value of 17.5%. In form II, there are three molecules in the asymmetric unit with the molecules related by a non-crystallographic  $3_2$  symmetry axis. In both crystal forms, it was found that only a few residues effectively participate in the formation of intermolecular contacts along both the crystallographic (form I) and the non-crystallographic (form II)  $3_2$  axes. The crystal structure of the form II crystal is compared with those of other rubredoxin molecules from anaerobic bacteria. From this comparison, a similarity in the core region, which is composed of aromatic residues and includes the active centre, has been revealed.

Received 18 April 1998  
Accepted 15 September 1998

**PDB References:** form I  
rubredoxin, 1rdv; form II  
rubredoxin, 2rdv.

## 1. Introduction

Rubredoxins and ferredoxins are known as non-haem iron proteins which function as electron carriers for the various enzymes. In ferredoxins, Fe atoms along with two or four labile S atoms form a cluster, whereas in rubredoxins only a single Fe atom is simply coordinated by four S atoms from cysteine residues. There have been two reports which describe the possible electron-transfer partners for rubredoxin molecules. The rubredoxin from *Pseudomonas oleovorans* has been implicated in the electron-transfer pathway for the  $\omega$ -hydroxylation of alkanes and fatty acids in the presence of NADH and O<sub>2</sub> (Peterson & Coon, 1968), whereas the rubredoxin from *Desulfovibrio gigas* was reported to act as an electron donor to a flavohaemoprotein, rubredoxin–oxygen oxidoreductase (Chen *et al.*, 1993). In contrast, the physiological role of the rubredoxins from other sulfate-reducing bacteria has not yet been elucidated. The rubredoxin from *D. vulgaris* Miyazaki F (RdDvMF) has been reported to have a role as an electron acceptor for the intracellular lactate dehydrogenase in collaboration with naphthoquinone. In this reaction, an electron extracted from lactate would be transferred to the network of electron-carrier proteins to effect electron-transfer-coupled phosphorylation (Shimizu *et al.*, 1989). RdDvMF is composed of 52 amino-acid residues and is highly homologous to the rubredoxin from *D. vulgaris* Hildenborough (RdDvH; Bruschi, 1976a). In order to establish the role of the invariant and/or variant residues between RdDvH and RdDvMF, and the universal relationships between the function and the structure of the rubredoxin

**Table 1**

Data statistics of the rubredoxin crystals in form I and form II from *D. vulgaris* Miyazaki F.

	Form I	Form II
Molecular weight	5574	5574
Number of residues	52	52
Crystal system	Trigonal	Monoclinic
Space group	$P3_221$	$P2_1$
$a$ (Å)	43.7	27.3
$b$ (Å)	43.7	44.9
$c$ (Å)	50.7	51.2
$\gamma$ or $\beta$ (°)	120.0	90.6
$V$ (Å <sup>3</sup> )	83850	62665
$Z$	6	6
$V_M$ (Å <sup>3</sup> Da <sup>-1</sup> )	2.51	1.87
Resolution (Å)	2.0	1.9
Total number of measured reflections	10630	53316
Total number of unique reflections (>3 $\sigma$ )	2541	9604
Completeness (%)	53.6	82.5
$R_{\text{merge}}$ (%)	8.9	11.1
$R$ ( $R_{\text{free}}^\dagger$ ) (%)	20.8 (27.2)	17.5 (21.6)
Number of water molecules	32	86
Mean $B$ factors (all atoms) (Å <sup>2</sup> )	38.0	14.1
Mean $B$ factors (water) (Å <sup>2</sup> )	50.8	31.7
R.m.s. $\Delta B$ factors for bonded atoms (Å <sup>2</sup> )	3.3	2.3

$^\dagger R_{\text{free}}$  values (Brünger, 1992b) were calculated with 5% of the total structure factors, which were not included in the process of the structure refinement.

molecule, crystallographic structure determination of RdDvMF has been carried out.

## 2. Methods and materials

### 2.1. Data collection and processing

The rubredoxin was extracted and purified according to the method previously described (Shimizu *et al.*, 1989). The crystals were grown in two crystal forms (form I,  $P3_221$  with unit-cell dimensions of  $a = b = 43.7$ ,  $c = 50.7$  Å; form II,  $P2_1$  with  $a = 27.3$ ,  $b = 44.9$ ,  $c = 51.2$  Å and  $\beta = 90.6^\circ$ ; Higuchi *et al.*, 1998). X-ray data collection was carried out with a Weissenberg camera for macromolecular crystallography using synchrotron radiation of wavelength 1.00 Å on two beamlines (BL-6A and BL-18B) at the Photon Factory of the National Laboratory for High Energy Physics in Tsukuba, Japan. Diffraction data were collected from a single crystal for form I and from three crystals for form II. Diffraction patterns were recorded on Fuji imaging plates and scanned images were obtained using a BA-100 system. The intensity data were processed using the *WEIS* (Higashi, 1989) and *PROTEIN* (Steigemann, 1992) program packages for the form I crystal and using the *DENZO* and *SCALEPACK* (Otwinowski, 1993) for the form II crystal. The data-processing statistics are shown in Table 1.

### 2.2. Structure determination

The structure of the form I crystal was solved by the molecular-replacement method using the *X-PLOR* program package (Brünger, 1992a). Molecular replacement was first implemented for form I because the number of molecules in the asymmetric unit was expected to be one from its crystal data. The atomic coordinates of RdDvH reported at 1.5 Å resolution in the Protein Data Bank were used as a starting

**Table 2**

Stereochemical geometry of the refined structure of the rubredoxin in two crystal forms.

The structures of the two crystal forms with all protein atoms were checked using *PROCHECK* (Laskowski *et al.*, 1993).

Ramachandran plot	Form I ( $P3_221$ )	Form II ( $P2_1$ )
Number of non-Pro and Gly residues	38	114
Most favoured areas (%)	81.6	91.2
Additional allowed areas (%)	18.4	8.8
Generously allowed areas (%)	0.0	0.0
Disallowed areas (%)	0.0	0.0
Number of unfavoured Pro and Gly residues (total)	0 (12)	0 (36)
Main-chain stereochemistry		
Bond lengths (% favoured)	98.5	98.7
Bond angles (% favoured)	91.9	90.1
Planarity std $^\dagger$ (°)	1.6	1.4
Bad contacts (%)	7.7	7.7
$\alpha$ tetrahedral distortion std $^\dagger$ (°)	2.2	2.1
Hydrogen-bond energy std $^\dagger$	0.9	0.9
Number of <i>cis</i> -prolines (total)	0 (7)	0 (21)
Side-chain stereochemistry		
Number of unfavoured $\chi_1 - \chi_2$ plots (total)	1 (23)	0 (69)
$\chi_1$ torsion angles std $^\dagger$ (°)	18.2	11.3
$\chi_2$ <i>trans</i> torsion angles std $^\dagger$ (°)	21.4	13.5
Total statistics		
Planarity (% favoured)	83.3	91.7
Overall $G$ factors	0.01	0.24

$^\dagger$  Std = standard deviation.

model (Adman *et al.*, 1991). The initial  $R$  value for the molecular-replacement solution obtained from the cross-rotation and translation search was 43.4%, using 941 reflections in the 6–3 Å resolution range. This  $R$  value is about 10% lower than those of the other possible solutions. Following rigid-body refinement, the  $R$  value decreased to 39.4% and side-chain atoms were fitted into the  $2|F_o| - |F_c|$  electron-density map. The structure was further refined to an  $R$  value of 24.3% (2066 reflections in the resolution range 6–2.5 Å) using the simulated-annealing method implemented in *X-PLOR*. After the placement and refinement of 32 water molecules, the  $R$  value was reduced to 20.8% (2541 reflections in the resolution range 6–2.0 Å). The resulting structure determined for form I was used as a molecular-replacement model in the determination of the form II crystal structure. The self-rotation function for form II suggested that the crystal contained three molecules in the asymmetric unit. One of the three molecules in the asymmetric unit was easily positioned from a rotation and translation search. The remaining two molecules were successively located in  $2|F_o| - |F_c|$  electron-density maps calculated with phases obtained from the previously positioned molecules. These three molecules were refined independently without imposing non-crystallographic symmetry restraints. The initial  $R$  values following the placement of one, two and all three molecules in the asymmetric unit were 49.6, 42.0 and 34.5%, respectively. The  $R$  value converged to 17.4% (6.0–1.9 Å, 9604 reflections) with the inclusion of 86 water molecules. The structure-determination statistics are listed in Table 1.

**Table 3**

R.m.s. distances (Å) between known structures of various rubredoxins (Å).

	Main-chain atoms (all atoms)			Main-chain atoms				
	DvMF†			DvH†	Dg†	Dd†	Pf†	Cp†
	P2 <sub>1</sub> -2‡	P2 <sub>1</sub> -3‡	P3 <sub>2</sub> 21§					
P2 <sub>1</sub> -1‡	0.51 (0.94)	0.52 (0.81)	0.55 (0.94)	0.57	0.73	0.76¶	0.73	0.56
P2 <sub>1</sub> -2‡		0.33 (0.72)	0.35 (0.77)	0.46	0.71	0.68¶	0.53	0.41
P2 <sub>1</sub> -3‡			0.37 (0.81)	0.47	0.63	0.77¶	0.53	0.33
P3 <sub>2</sub> 21§				0.52	0.72	0.83¶	0.62	0.47
DvH†					0.71	0.64¶	0.61	0.56
Dg†						0.78¶	0.75	0.53
Dd†							0.76	0.74
Pf†								0.47

‡ Three rubredoxin molecules related by a non-crystallographic 3<sub>2</sub> symmetry in the form II crystal of *D. vulgaris* Miyazaki F. § Rubredoxin molecule in the form I crystal of *D. vulgaris* Miyazaki F. † DvMF, DvH, Dg, Dd, Pf, Cp: rubredoxin molecules from *Desulfovibrio vulgaris* Miyazaki F, *D. vulgaris* Hildenborough, *D. gigas*, *D. desulfuricans* strain 27774, *Pyrococcus furiosus* and *Clostridium pasteurianum*, respectively. ¶ Small loop regions which correspond to Asp19–Lys25 in DvMF rubredoxin were omitted from the calculation.

### 3. Results and discussion

#### 3.1. Molecular structure and crystal packing

The molecular size of RdDvMF is approximately 23 × 28 × 20 Å. The stereochemical quality of the refined structures in both form I and form II was verified using the program *PROCHECK* (Laskowski *et al.*, 1993), which showed quite favourable agreement with known stereochemical properties of proteins (Table 2). *B* factors of the protein atoms and root-mean-square Δ of *B* factors for bonded atoms also converged

in both the molecular structures (Table 1). There is only one molecule in the asymmetric unit of the form I crystal. On the other hand, the asymmetric unit of the form II crystal contains three molecules related by a non-crystallographic 3<sub>2</sub> symmetry axis which sits along the crystallographic *c* axis and is illustrated in Fig. 1. This pseudo 3<sub>2</sub> symmetry was deduced from the intensity pattern of the low-resolution reflections along the *c*\* axis. The r.m.s. deviations for all protein atoms between each pair of crystallographically independent molecules in two crystal forms of RdDvMF (that is, one molecule in form I and

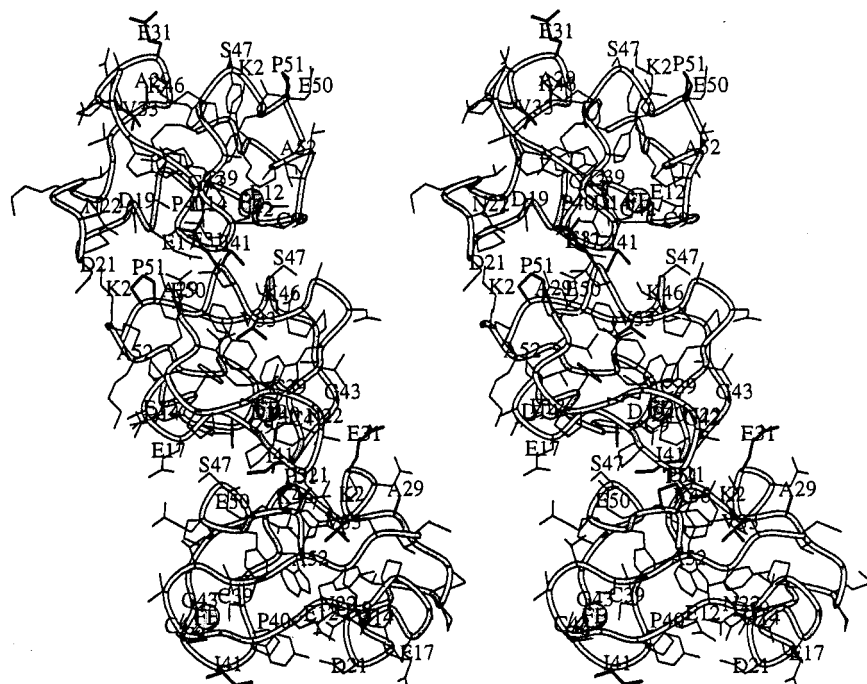


**Figure 1**

A stereoview along the *b* axis showing non-crystallographic 3<sub>2</sub> symmetry-related rubredoxin molecules from *D. vulgaris* Miyazaki F in the form II crystal. The main-chain folding is shown as a coil and the Fe atom at the active site is represented by a sphere. Non-conserved residues which are substituted in the rubredoxin of the strain Hildenborough (Ala29, Glu31, Val33, Ile41 and Pro51) are indicated with thick lines. Glu31, Ile41 and Pro51 effectively participate in the formation of the real (form I) and the pseudo (form II) 3<sub>2</sub>-symmetry axes along the crystallographic *c* axis. The residues which participate in the intermolecular interactions are numbered with the one-letter amino-acid code. The figure was produced using the program *MOLSCRIPT* (Kraulis, 1991).

three molecules in form II) range between 0.7 and 1.0 Å (Table 3). This indicates that the three-dimensional structures are very similar for all the crystallographically independent molecules, even though there are quite striking differences between the crystal packing of the two crystal forms. In addition, the set of three molecules related by crystallographic 3<sub>2</sub> symmetry in the form I crystal can be superimposed onto the three molecules in the form II crystal which are related by the non-crystallographic 3<sub>2</sub> symmetry, with an r.m.s. deviation of 0.94 Å for all protein atoms. However, owing to the existence of additional crystallographic symmetry elements as well as the differences in the shape and size of the two crystal unit cells, both forms show unique crystal-packing structures. As a consequence, form I contains a large solvent cavity which contributes to a larger solvent content of 51% for form I *versus* 34% for form II (Figs. 2*a* and 2*b*). This is likely to contribute to the enhanced diffraction of form II compared with form I (Table 1).

#### 3.2. Intermolecular and intramolecular interactions

Fig. 3 shows the amino-acid sequence comparison between RdDvMF and rubredoxin molecules from various anaerobic

bacteria. As a consequence of the similarity of the amino-acid sequence, the r.m.s. deviations for main-chain atoms between the known structures of rubredoxin, RdDvMF, RdDvH, RdDg from *Desulfovibrio gigas* (Frey *et al.*, 1987), RdPf from *Pyrococcus furiosus* (Day *et al.*, 1992), RdCp from *Clostridium pasteurianum* (Watenpaugh *et al.*, 1973) and RdDd from *Desulfovibrio desulfuricans* strain 27774 (Stenkamp *et al.*, 1990) are all within 1.0 Å (Table 3). The degrees of similarity in both the overall folding pattern and the primary sequence are very high, with the exception of RdDd, which has a deletion in the site corresponding to the short loop Asp19–Lys25 in RdDvMF.

The sequence identities between three rubredoxin molecules from sulfate-reducing bacteria, RdDvMF, RdDvH and RdDg (Bruschi, 1976*b*) are calculated to be 90.4% (RdDvMF–RdDvH), 71.2% (RdDvMF–RdDg), and 73.1% (RdDvH–RdDg). From a comparison between RdDvMF and RdDvH, only five amino-acid substitutions were found (Fig. 3). Four of these substitutions, Ala29 (Ser29), Glu31 (Asp31), Ile41 (Val41) and Pro51 (Ala51) in RdDvMF (RdDvH) are located at the molecular surface, but Val33 (Leu33) is directed toward the core region of the molecule and is surrounded by aromatic side chains. The side chain of a valine residue is smaller than

that of a leucine residue, therefore Val33 can be located in this position without significant steric hindrance. However, the crystal packing of RdDvMF is different to that of RdDvH, even though both proteins show high sequence similarities and three-dimensional structural similarities. Crystals of RdDvH belong to the space group  $P2_1$ , which is the same as that of the form I crystal of RdDvMF, but non-crystallographic  $3_2$  symmetry does not exist in the RdDvH asymmetric unit. One interesting point is the relationship between RdDvH and RdDg. Though the sequence homology between RdDvH and RdDg is much lower than that between RdDvH and RdDvMF, RdDvH and RdDg exhibit common crystallographic and structural features, such as the space group of the crystal, unit-cell dimensions, molecular packing and the overall folding pattern.

From a careful examination of the three-dimensional structures of RdDvMF molecules in both crystal forms I and II, two types of interactions, hydrophobic interactions and hydrogen bonding, predominate along the interface between the three molecules related either by a real or a pseudo  $3_2$  symmetry axis (Table 4). The side-chain atoms of three substituted residues, Glu31, Ile41 and Pro51 make strong hydrophobic interactions with the side-chain and/or main-chain atoms of Tyr11, Asp21, Pro40, Ile41 and Cys42 of the neighbouring molecules. Among them, Ile41 C $^{\delta}$  and Pro51 C $^{\gamma}$  effectively lie along the real or the pseudo  $3_2$  symmetry axis. On the other hand, the side-chain atoms of Glu31 participate in the hydrogen-bonding network between  $3_2$  symmetry-related molecules and water molecules. Since the amino-acid substitution of the aspartate in RdDvH by the glutamate in RdDvMF at position 31 seems to have little effect on the surface structure of the molecule and most of the hydrogen bonds involve water molecules, the hydrophobic interactions involving the substituted amino acids (Ile41 and Pro51) serve the primary role in preserving the  $3_2$  symmetry in both the crystal structures.

Lys46, which participates in the hydrophilic interaction between neighbouring molecules (Table 4), is known to be one of the most strictly conserved residues among all rubredoxins (Fig. 3). The side-chain N atom of the lysine residue also forms intramolecular hydrogen bonds with the carbonyl O atoms of Phe30 and Val33. These two intramolecular hydrogen bonds also exist in other rubredoxins. As pointed out previously, this Lys46 seems to have a role in stabilizing the three-dimensional structure of the molecule (Sieker *et al.*, 1994).

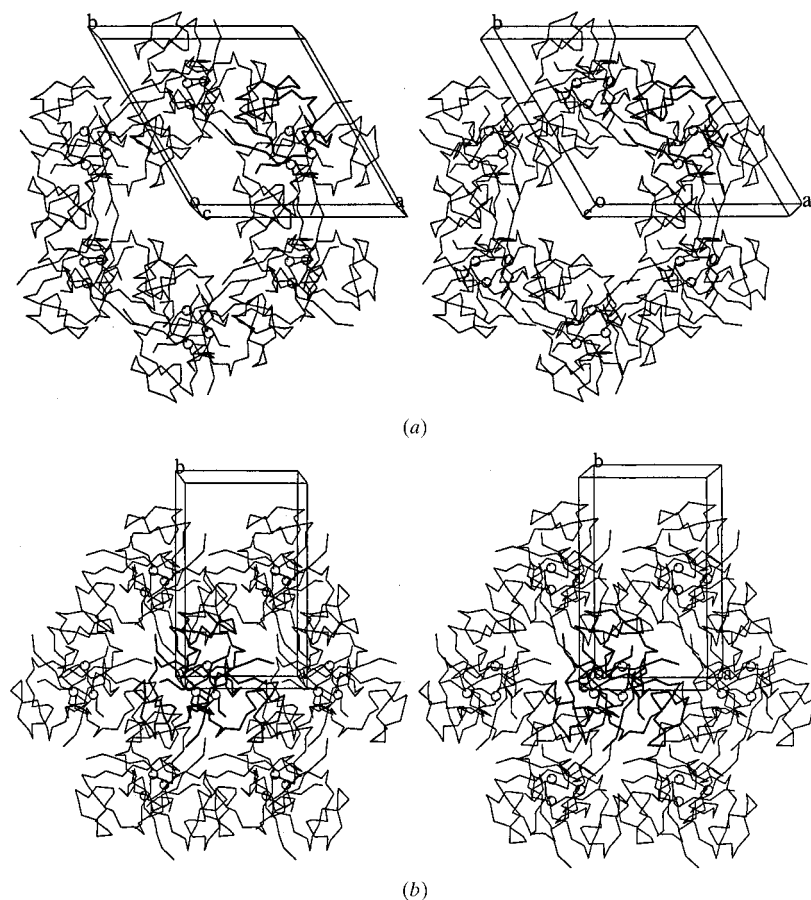


**Figure 2**  
Stereoviews of the crystal packings in (a) form I and (b) form II of the Miyazaki rubredoxin. Each set of three molecules related by a real (form I) or a pseudo (form II)  $3_2$  symmetry is packed uniquely in each crystal unit cell, resulting in the difference in solvent content between the two crystal forms. The figures were produced using the program MOLSCRIPT (Kraulis, 1991).

### 3.3. Metal centre

Fig. 4 shows a view of the central core part of the structure of the RdDvMF molecule in form II. The Fe atom is coordinated by four S atoms of

**Table 4**  
Interactions (<4.0 Å) among three molecules related by real (form I) and pseudo (form II) 3<sub>2</sub> symmetry in two crystal forms.

Hydrophobic interaction	
Atom	Atom of the nearest molecules
Glu31 C <sup>γ</sup>	Cys42 C, Cys42 O
Lys46 C <sup>ε</sup>	Ile41 C <sup>γ2</sup>
Ser47 C <sup>β</sup>	Tyr11 N, Tyr11 C <sup>α</sup> , Tyr11 C, Tyr11 O, Ile41 C <sup>δ</sup>
Pro51 C <sup>γ</sup>	Pro40 C <sup>β</sup>
Pro51 C <sup>β</sup>	Asp21 C <sup>β</sup>
Hydrophilic interaction (hydrogen bonding)	
Atom	Atom of the nearest molecules
Lys2 N <sup>ε</sup>	Asp21 O <sup>δ1</sup> , Asn22 N <sup>δ2</sup>
Tyr4 O <sup>γ</sup>	Pro40 O, Asn22 O <sup>δ1†</sup>
Glu31 O <sup>ε1</sup>	Gly43 O <sup>†</sup> , Cys39 O <sup>†</sup> , Pro40 O <sup>†</sup>
Lys46 N <sup>ε</sup>	Ile41 O
Ser47 O	Glu12 N, Glu12 O <sup>†</sup>
Ser47 O <sup>γ</sup>	Cys9 O <sup>†</sup>
Glu50 O <sup>ε1</sup> , Glu50 O <sup>ε2</sup>	Tyr11 O <sup>γ†</sup> , Asp19 O <sup>δ1†</sup> , Glu17 O <sup>ε1†</sup> , Gly18 O <sup>†</sup> , Asp14 N <sup>†</sup> , Glu12 O <sup>†</sup> , Asp21 N <sup>†</sup>
Ala52 O	Asp21 O <sup>δ2</sup>

† Interactions mediated by one or two water molecules.

	1	10	20	30	40	50
DvMF	MKKYVCTVCG	YEYDPAEGDP	DNGVKPGTGF	EDMPADWVCP	ICGAPKSEFE	EA
DvH	MKKYVCTVCG	YEYDPAEGDP	DNGVKPGTGF	EDMPADWVCP	ICGAPKSEFE	EA
Dg	MDIYVCTVCG	YEYDPAKGDG	DSGIKPGTKF	EDLPDDWACP	VCGASKDAFE	KQ
Pf	AKWVCKICG	YIYDEDAGDP	DNGISPPTKF	EELPDDWVCP	ICGAPKSEFE	KLED
Cp	MKKYTCTVCG	YIYDPEDGDP	DDGVNPGTDF	KDIPDDWVCP	LGVGKDEFE	EVEE
Dd	MQKYVCNVCG	YEYDPAEIH	DNVVF	DQLEDDWCCP	VCGVSKDQFS	PA

**Figure 3**  
Sequence comparison of rubredoxin molecules from anaerobic bacteria. The conserved residues are shaded and the substituted residues between RdDvMF and RdDvH are boxed. DvMF, *D. vulgaris* Miyazaki F; DvH, *D. vulgaris* Hildenborough (Bruschi, 1976a); Dg, *D. gigas* (Bruschi, 1976b); Pf, *Pyrococcus furiosus* (Blake *et al.*, 1991); Cp, *Clostridium pasteurianum* (Herriott *et al.*, 1973); Dd, *D. desulfuricans* (Hormel *et al.*, 1986).

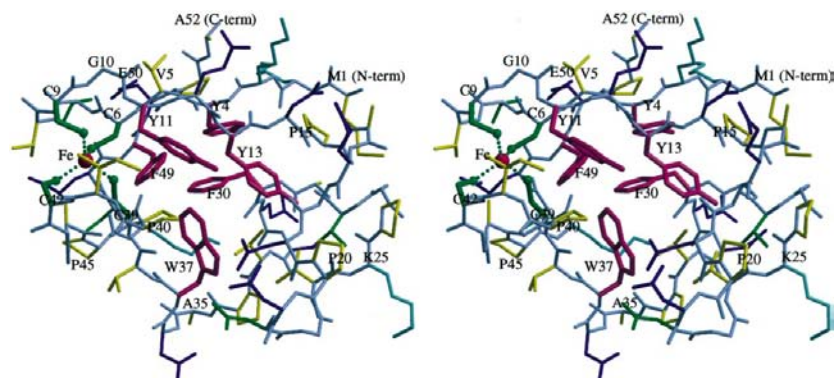


**Figure 4**  
A stereoview of the hydrophobic core centre of the Miyazaki rubredoxin in the form II crystal. The conserved aromatic residues, the coordinated four cysteine residues and every five residues are numbered with a one-letter code. The side-chain atoms of the aromatic, hydrophobic, basic, acidic and neutral residues are coloured pink, yellow, blue, cyan and green, respectively. Main-chain atoms are coloured grey and the Fe atom is shown as a purple sphere. The figure was produced using the programs *MOLSCRIPT* and *RASTER-3D* (Kraulis, 1991; Merritt & Murphy, 1994).

cysteine residues Cys6, Cys9, Cys39 and Cys42. The distances between the ligand S<sup>γ</sup> atoms and the Fe atom are in the range 2.29–2.33 Å. They are similar to the average values of the Fe–S distances (2.29 Å) found in other rubredoxins, but shorter than the Zn–S bond length (2.35 Å) in the Zn-substituted rubredoxin (Dauter *et al.*, 1996). There are no significant differences in the coordination geometry among the four RdDvMF molecules (three molecules related by the non-crystallographic 3<sub>2</sub> symmetry in form II and one molecule in form I). The lengths of hydrogen bonds between the S<sup>γ</sup> atoms of the *i*th ligand cysteine residues and the peptide N atoms of the (*i* + 2)nd or (*i* + 3)rd residues in the four RdDvMF molecules in forms I and II range from 3.40 to 3.69 Å. Within a single RdDvMF molecule, no special features such as a twofold symmetry relationship between the bond lengths of the hydrogen bonds (S<sup>γ</sup>–H–N) can be found. Since the structure around the Fe atom (not only the Fe atom and coordinated cysteine S atoms, but also the peptide N atoms which hydrogen bond to the S atoms) is quite highly conserved among all the known rubredoxin structures, this region of the rubredoxin molecule is likely to be essential for function.

### 3.4. Hydrophobic core centre

Five conserved aromatic residues, Tyr4, Tyr13, Trp37 and Phe49, are located within the hydrophobic core of the structure near the active centre (Fig. 4). Though Tyr4 of RdDvMF is not strictly conserved in other rubredoxins (Fig. 3), all of the known rubredoxins have an aromatic residue at this position in the sequence. This conservation of aromatic residues is involved in the formation of a shape similar to the so-called ‘donut’ structure, and this shape should be essential for the function of rubredoxin molecules. The Fe atom itself is surrounded by –Cys6–Thr–Val–Cys9– and –Cys39–Pro–Ile–Cys42–. These turn regions also surround the Fe atoms in other rubredoxin structures. Therefore, the Fe atom is not directly accessible from the surface of the molecule (Watenpaugh *et al.*, 1980). Since the two coordinated cysteine residues (Cys6 and Cys39) are located within 4.0 Å of the two of the aromatic residues (Phe49 and Tyr11), it is possible to form an interaction between the Fe atom and these aromatic two residues. This central core part composed of the aromatic residues is accessible from both sides of the molecule (Fig. 4). It is proposed that one side of

the molecule interacts with electron-donor proteins to receive an electron and the other side of the molecule interacts with electron-acceptor proteins to give up an electron.

## References

- Adman, E. T., Sieker, L. C. & Jensen, L. H. (1991). *J. Mol. Biol.* **217**, 337–352.
- Blake, P. R., Park, J. B., Bryant, F. O., Aono, S., Magnuson, J. K., Eccleston, E., Howard, J. B., Summers, M. F. & Adams, M. W. W. (1991). *Biochemistry*, **30**, 10885–10895.
- Brünger, A. T. (1992a). *X-PLOR, Version 3.1. A System for X-ray Crystallography and NMR*. Yale University Press, New Haven, USA.
- Brünger, A. T. (1992b). *Nature (London)*, **355**, 472–474.
- Bruschi, M. (1976a). *Biochim. Biophys. Acta*, **434**, 4–17.
- Bruschi, M. (1976b). *Biochem. Biophys. Res. Commun.* **70**, 615–621.
- Chen, L., Liu, M.-Y., LeGall, J., Fareleira, P., Santos, H. & Xavier, A. V. (1993). *Biochem. Biophys. Res. Commun.* **193**, 100–105.
- Dauter, Z., Wilson, K. S., Sieker, L. C., Moulis, J. M. & Meyer, J. (1996). *Proc. Natl Acad. Sci. USA*, **93**, 8836–8840.
- Day, M. W., Hsu, B. T., Joshua-Tor, L., Park, J. B., Zhou, Z. H., Adams, M. W. & Rees, D. C. (1992). *Protein Sci.* **11**, 1494–1507.
- Frey, M., Sieker, L., Payan, F., Haser, R., Bruschi, M., Pepe, G. & LeGall, J. (1987). *J. Mol. Biol.* **197**, 525–541.
- Herriott, J. R., Watenpaugh, K. D., Sieker, L. C. & Jensen, L. H. (1973). *J. Mol. Biol.* **80**, 423–432.
- Higashi, T. (1989). *J. Appl. Cryst.* **18**, 129–130.
- Higuchi, Y., Misaki, S., Sugiyama, S., Morimoto, Y., Ogata, M., Yagi, T. & Yasuoka, N. (1998). *Protein Pept. Lett.* **5**, 175–176.
- Hormel, S., Walsh, K. A., Prickril, B. C., Titani, K., LeGall, J. & Sieker, L. C., (1986). *FEBS Lett.* **201**, 147–150.
- Kraulis, P. J. (1991). *J. Appl. Cryst.* **24**, 946–950.
- Laskowski, R. A., MacArthur, M. W., Moss, D. S. & Thornton, J. M. (1993). *J. Appl. Cryst.* **26**, 283–291.
- Merritt, E. A. & Murphy, M. E. (1994). *Acta Cryst.* **D50**, 869–873.
- Otwinowski, Z. (1993). *Data Collection and Processing. Proceedings of the CCP4 Study Weekend*, edited by L. Sawyer, N. Isaacs & S. Bailey, pp. 56–62. Warrington: Daresbury Laboratory.
- Peterson, J. A. & Coon, M. J. (1968). *J. Biol. Chem.* **243**, 329–334.
- Shimizu, F., Ogata, M., Yagi, T., Wakabayashi, S. & Matsubara, H. (1989). *Biochimie*, **71**, 1171–1177.
- Sieker, L. C., Stenkamp, R. E. & LeGall, J. (1994). *Methods Enzymol.* **243**, 203–216.
- Steigemann, W. (1992). *PROTEIN, Version 3.1. A Program System for the Crystal Structure Analysis of Proteins*. Max-Planck Institute für Biochemie, Martinsried, Germany.
- Stenkamp, R. E., Sieker, L. C. & Jensen, L. H. (1990). *Proteins*, **8**, 352–364.
- Watenpaugh, K. D., Sieker, L. C., Herriott, J. R. & Jensen, L. H. (1973). *Acta Cryst.* **B29**, 943–956.
- Watenpaugh, K. D., Sieker, L. C. & Jensen, L. H. (1980). *J. Mol. Biol.* **138**, 615–633.